

## A CELESTIAL GAMMA-RAY FOREGROUND DUE TO THE ALBEDO OF SMALL SOLAR SYSTEM BODIES AND A REMOTE PROBE OF THE INTERSTELLAR COSMIC-RAY SPECTRUM

IGOR V. MOSKALENKO<sup>1</sup>

Hansen Experimental Physics Laboratory, Stanford University, Stanford, CA 94305; imos@stanford.edu

TROY A. PORTER

Santa Cruz Institute for Particle Physics, University of California, Santa Cruz, CA 95064; tporter@scipp.ucsc.edu

SETH W. DIGEL<sup>1</sup>

Stanford Linear Accelerator Center, 2575 Sand Hill Road, Menlo Park, CA 94025; digel@stanford.edu

PETER F. MICHELSON<sup>1</sup>

Department of Physics, Stanford University, Stanford, CA 94305; peterm@stanford.edu

AND

JONATHAN F. ORMES

Department of Physics and Astronomy, University of Denver, Denver, CO 80208; jormes@du.edu

Received 2007 December 6; accepted 2008 March 15

### ABSTRACT

We calculate the  $\gamma$ -ray albedo flux from cosmic-ray (CR) interactions with the solid rock and ice in Main Belt asteroids (MBAs), Jovian and Neptunian Trojan asteroids, and Kuiper Belt objects (KBOs) using the Moon as a template. We show that the  $\gamma$ -ray albedo for the Main Belt, Trojans, and Kuiper Belt strongly depends on the small-body size distribution of each system. Based on an analysis of the Energetic Gamma-Ray Experiment Telescope (EGRET) data we infer that the diffuse emission from the MBAs, Trojans, and KBOs has an integrated flux of less than  $\sim 6 \times 10^{-6} \text{ cm}^{-2} \text{ s}^{-1}$  (100–500 MeV), which corresponds to  $\sim 12$  times the lunar albedo, and may be detectable by the forthcoming *Gamma-Ray Large Area Space Telescope (GLAST)*. If detected by *GLAST*, it can provide unique direct information about the number of small bodies in each system that is difficult to assess by any other method. In addition, the KBO albedo flux can be used to probe the spectrum of CR nuclei at close-to-interstellar conditions. The orbits of MBAs, Trojans, and KBOs are distributed near the ecliptic, which passes through the Galactic center and high Galactic latitudes. Therefore, the asteroid  $\gamma$ -ray albedo has to be taken into account when analyzing weak  $\gamma$ -ray sources close to the ecliptic, especially near the Galactic center, and signals at high Galactic latitudes, such as the extragalactic  $\gamma$ -ray emission. The asteroid albedo spectrum also exhibits a 511 keV line due to secondary positrons annihilating in the rock. This may be an important and previously unrecognized celestial foreground for the *International Gamma-Ray Astrophysics Laboratory (INTEGRAL)* observations of the Galactic 511 keV line emission including the direction of the Galactic center.

*Subject headings:* cosmic rays — elementary particles — Galaxy: bulge — gamma rays: theory — Kuiper Belt — minor planets, asteroids

*Online material:* color figure

### 1. INTRODUCTION

The populations of small solar system bodies (SSSBs) in the asteroid belt between Mars and Jupiter, Jovian and Neptunian Trojans, and SSSBs in the Kuiper Belt beyond Neptune’s orbit (often called also trans-Neptunian objects, TNOs) remain the least explored members of the solar system. A majority of the MBAs and KBOs have their orbits distributed near the ecliptic with a FWHM of the order of  $10^\circ$  in ecliptic latitude (Binzel et al. 1999; Brown 2001). The spatial and size distributions of these objects provide important information about the dynamical evolution of the solar system. Extending our knowledge of the size distribution of these objects below the current subkilometer size limits of optical (e.g., Ivezić et al. 2001; Wiegert et al. 2007) and infrared (e.g., Tedesco & Desert 2002; Yoshida et al. 2003) measurements would provide additional information on the accretion/collision and depletion processes that formed the populations of

SSSBs.<sup>2</sup> In this paper we show that the CR-induced  $\gamma$ -ray albedo of these systems may be bright enough to be detected with a  $\gamma$ -ray telescope such as *GLAST*, *INTEGRAL*, and/or the Soft Gamma-ray Detector (SGD) aboard the *NeXT* satellite (Takahashi et al. 2006), and can allow us to probe the size distribution of SSSBs down to a few meters. In addition, the  $\gamma$ -ray emission of these systems may comprise a “diffuse”  $\gamma$ -ray foreground that should be taken into account when evaluating the flux and spectra of  $\gamma$ -ray sources near the ecliptic. Our preliminary results are presented in Moskalenko et al. (2008).

The Galactic center is a region crowded with  $\gamma$ -ray sources and is one of the preferred places to look for  $\gamma$ -ray signatures of dark matter (DM). Extensive literature on the subject exists (e.g., Bergström et al. 1998; Zaharijas & Hooper 2006; Finkbeiner & Weiner 2007; Hooper et al. 2008; Baltz et al. 2008; also references in these papers). The ecliptic crosses the Galactic equator near the

<sup>1</sup> Also at: Kavli Institute for Particle Astrophysics and Cosmology, Stanford University, Stanford, CA 94309.

<sup>2</sup> We note that Babich et al. (2007) have suggested a method to place constraints on the mass, distance, and size distribution of TNOs using spectral distortions of the cosmic microwave background.



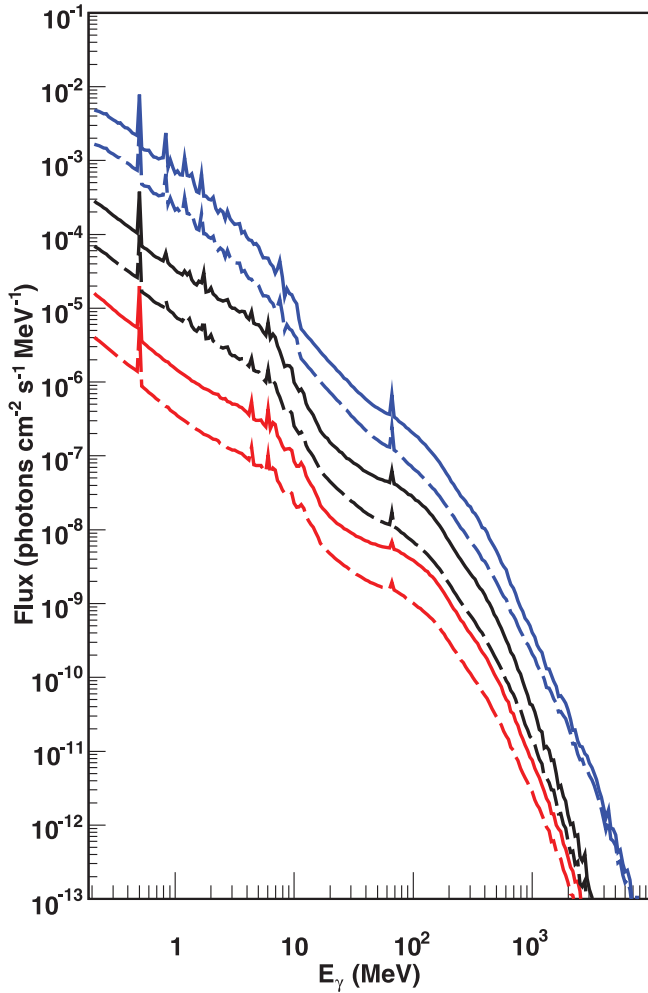


FIG. 3.— Calculated  $\gamma$ -ray albedo spectrum of a Moon-sized body at the lunar distance composed of Moon rock (*black lines*), iron ( $\times 10$ , *blue lines*), and water ice ( $\times 0.1$ , *red lines*). Solid lines show the cases for no modulation, long-dashed lines for  $\Phi = 1500$  MV.

different materials are considerably different, and the nuclear emission lines can be used to distinguish between the materials. The high-energy parts are essentially featureless and have similar shape. The flux between iron and water ice changes by a factor of  $\sim 2$  above 100 MeV with the latter producing the larger flux. Above  $\sim 100$  MeV the regolith albedo approaches the water ice albedo.

The 511 keV line in Figures 2 and 3 is due to the annihilation of positrons produced by CR cascades in the solid target (iron, regolith, or ice). In Figure 2, the albedo spectrum also includes the contribution by CR positrons in the lunar rock target (see below). Since the rock is solid, secondary positrons quickly thermalize and produce a narrow annihilation line. Its width is determined by the energy bin size adopted in the simulation.

Figure 4 shows the components of the albedo spectrum (Fig. 2) below 20 MeV. The thick solid lines show the total albedo flux due to the CR proton, helium, and positron interactions with regolith for no modulation (*red thick solid line*) and a modulation level of 1500 MV (*blue thick solid line*). The thin solid lines show the albedo spectrum due to CR positron interactions with regolith for the same cases of no modulation (*red thin solid line*) and a modulation level of 1500 MV (*blue thin solid line*). The dashed and dotted lines show the components of the CR positron induced  $\gamma$ -rays, from the center and the rim, respectively.

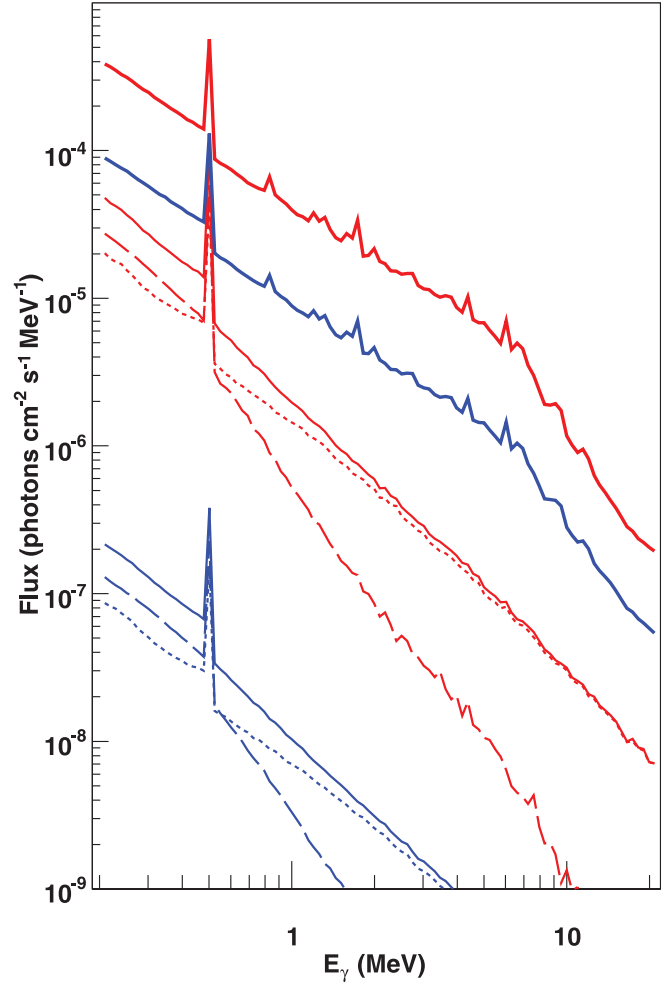


FIG. 4.— Calculated  $\gamma$ -ray albedo spectrum showing components below 20 MeV for no modulation (*red lines*) and modulation level 1500 MV (*blue lines*). *Long-dashed lines*, positron-induced  $\gamma$ -rays from center; *short-dashed lines*, CR positron induced  $\gamma$ -rays from rim; *thin solid lines*, total CR positron induced  $\gamma$ -rays; *thick solid lines*, total  $\gamma$ -ray emission from CR positrons and nucleons.

#### 4. ANALYSIS OF THE EGRET DATA

The EGRET instrument on the *Compton Gamma Ray Observatory* (1991–2000) surveyed the sky in the range  $>30$  MeV, and here we use the EGRET data together with the information in the Third EGRET Source Catalog (3EG; Hartman et al. 1999) to set limits on the signal from the SSSBs. Challenges to detecting diffuse emission associated with the ecliptic plane include the brightness of the Galactic diffuse emission (e.g., Hunter et al. 1997), the presence of bright point sources, the limited angular resolution and photon statistics of the EGRET data, and potential large-scale artifacts in the exposure maps owing to aging of the spark chamber gas.

We made maps of the EGRET data in ecliptic coordinates for Cycles 1–4 of the mission, during which most of the EGRET exposure was obtained. The event data, after standard cuts on zenith angle and inclination angle ( $30^\circ$ ), were binned on a photon-by-photon basis in ecliptic coordinates. The exposure maps for each EGRET viewing period were transformed into ecliptic coordinates and added together, and intensity maps were calculated from the photon and exposure maps.

In order to limit contributions from Galactic diffuse emission to any possible enhancement of diffuse intensity at low ecliptic latitudes, the region  $|b| < 20^\circ$  for  $|\ell| < 90^\circ$  and  $|b| < 10^\circ$  for

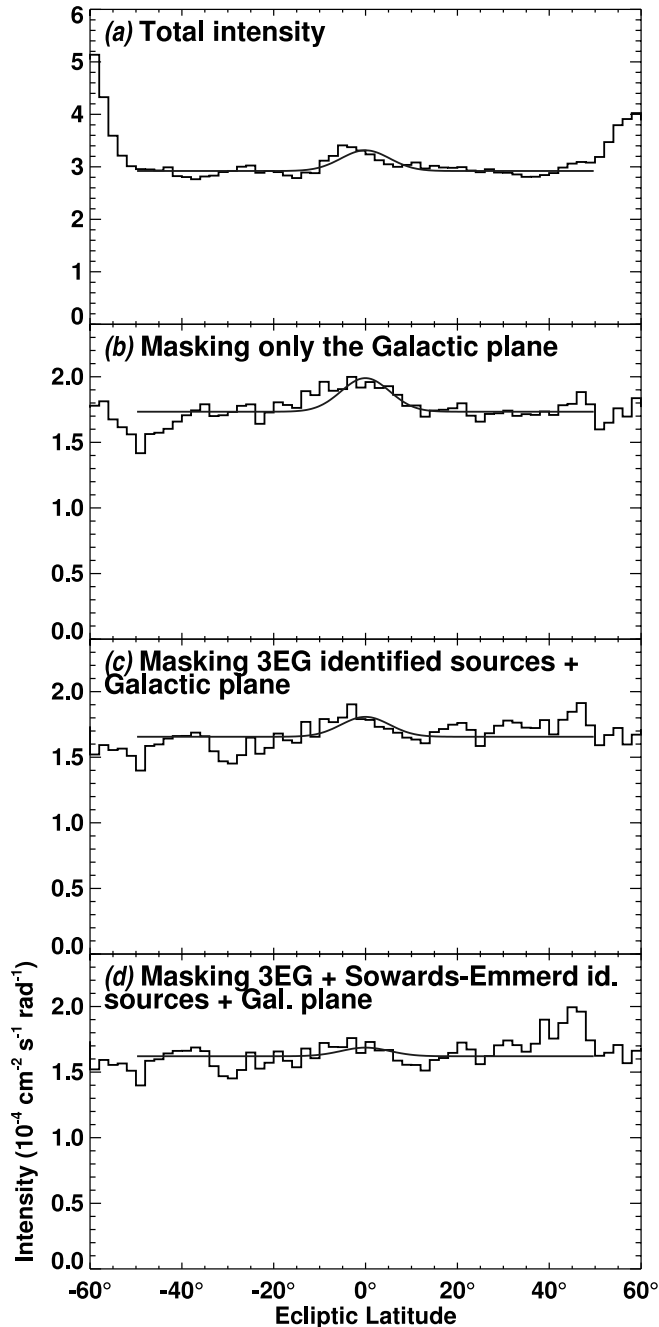


FIG. 5.—Profiles of  $\gamma$ -ray intensity with  $\beta$  derived from EGRET data as described in the text. The energy range is 100–500 MeV, and the profiles have been averaged over all ecliptic longitudes. (a) Profile derived with no masking of Galactic diffuse emission or  $\gamma$ -ray point sources. (b) Profile with the Galactic plane ( $|b| < 10^\circ$  for  $|\ell| > 90^\circ$  and  $|b| < 20^\circ$  for  $|\ell| < 90^\circ$ ) excluded. (c) Profile with the identified 3EG sources (Hartman et al. 1999) and the Galactic plane excluded. (d) Profile with the identified 3EG sources plus the further blazar identifications proposed by Sowards-Emmerd et al. (2003, 2004) excluded. Overlaid on each profile is the best-fitting Gaussian (12.5° FWHM, centered on  $\beta = 0$ ) plus a constant, fitted for the region  $|\beta| < 50^\circ$ . This approximates the distribution of albedo  $\gamma$ -ray emission expected for the KBO. [See the electronic edition of the Journal for a color version of this figure.]

$|\ell| > 90^\circ$  was masked out in the analysis. We also removed regions  $12^\circ$  in diameter around the position of each identified source in the 3EG catalog (designation other than “u” in the 3EG catalog).

Figure 5 presents the profile of  $\gamma$ -ray intensity in the 100–500 MeV range over ecliptic longitude. This range was chosen as having the brightest expected albedo emission in the energy range

of EGRET. As described in the figure legend, a sequence of profiles is shown for different combinations of the masks described above. In the last profile (Fig. 5d), the 3EG sources subsequently identified by Sowards-Emmerd et al. (2003, 2004) as likely to be blazars were included with the sources identified in the 3EG catalog in defining the mask. We did not mask out unidentified point sources because of the possibility that some of them may have represented detections of the  $\gamma$ -ray albedo from the Trojan groups, which move collectively, or fluctuations in the SSSB  $\gamma$ -ray albedo at low ecliptic latitudes.

In order to estimate the possible “excess” diffuse flux from MBAs, Trojans, and KBOs we calculated the integrated fluxes for ecliptic latitudes  $|\beta| < 15^\circ$  and all ecliptic longitudes (Table 1, “Flux” column). In order to increase the sensitivity and to search for a diffuse signal that is centered on the ecliptic, Table 1 also includes fluxes for the best-fitting Gaussian centered on  $\beta = 0^\circ$  and having FWHM width  $12.5^\circ$  (“Fitted Flux” column), the approximate extent of the Kuiper Belt (Brown 2001). The fits included a constant term to account for Galactic and extragalactic diffuse emission; profiles of the fits are included in Figure 5. The effective point-spread function (PSF) for EGRET in the 100–500 MeV range for the expected spectrum of the albedo emission is approximately  $4^\circ$  FWHM, which would not appreciably broaden the apparent distribution of  $\gamma$ -ray intensity. In any case, the assumption of a single Gaussian profile is an approximation; the contribution from MBAs should result in an additional somewhat narrower but fainter component to the diffuse emission around the ecliptic.

Gamma-ray emission associated with the Moon and Sun also contributes to the intensity of the sky at low ecliptic latitudes. The Moon is always within about  $5^\circ$  of the ecliptic, and the profiles shown in Figure 5 undoubtedly include lunar albedo  $\gamma$ -ray emission, at a level of  $\sim 5 \times 10^{-7} \text{ cm}^{-2} \text{ s}^{-1}$  (Moskalenko & Porter 2007). As described by Moskalenko et al. (2006) the solar radiation field is a fairly bright and diffuse  $\gamma$ -ray source from inverse Compton scattering of CR electrons. The solar inverse Compton emission is brightest in the ecliptic plane but of course depends on solar elongation angle. The precise contribution to the diffuse intensity at low ecliptic latitudes is difficult to estimate. The Sun was in the field of view of EGRET for only a small fraction of the observing time, and the contribution to the total flux should have been less than that of the Moon.

After the bright diffuse emission and identified point sources are masked from the EGRET data, no strong excess of diffuse emission is apparent at low ecliptic latitudes in Figure 5. The integrated fluxes are formally significant for the case where the Galactic plane and all sources identified in the 3EG catalog are masked out (Table 1; Fig. 5c), but the systematic uncertainties are comparable to the measurement. This is suggested by the effect on the integrated flux from masking out several more sources that Sowards-Emmerd et al. (2003, 2004) identified as blazars (Fig. 5d). The overall average exposure does not change appreciably as a result of the additional masking, but the fitted flux decreased by more than 50% (Table 1).

Based on our analysis of the EGRET data we infer that the diffuse emission from MBAs, Trojans, and KBOs has an integrated flux of less than  $\sim 6 \times 10^{-6} \text{ cm}^{-2} \text{ s}^{-1}$  (100–500 MeV), as derived from the set of cuts  $b$ , which corresponds to  $\sim 12$  lunar albedo flux units.

## 5. DISCUSSION AND CONCLUSION

The albedo  $\gamma$ -ray flux from MBAs can be calculated using equations (7)–(11) and Figures 2 and 3, where we assume that their surface material is regolith. We use the following parameters:

TABLE 1  
DIFFUSE INTENSITY AROUND THE ECLIPTIC (100–500 MeV)

SET OF CUTS IN FIGURE 5	$ \beta  < 15^\circ$			
	Flux ( $\text{cm}^{-2} \text{s}^{-1}$ )	Statistical Error	FITTED FLUX ( $\text{cm}^{-2} \text{s}^{-1}$ )	STATISTICAL ERROR
<i>a</i> .....	$1.006 \times 10^{-5}$	$5.5 \times 10^{-7}$	$9.16 \times 10^{-6}$	$3.5 \times 10^{-7}$
<i>b</i> .....	$7.95 \times 10^{-6}$	$5.8 \times 10^{-7}$	$5.95 \times 10^{-6}$	$3.7 \times 10^{-7}$
<i>c</i> .....	$3.59 \times 10^{-6}$	$6.7 \times 10^{-7}$	$3.53 \times 10^{-6}$	$4.4 \times 10^{-7}$
<i>d</i> .....	$1.1 \times 10^{-7}$	$7.4 \times 10^{-7}$	$1.52 \times 10^{-6}$	$5.1 \times 10^{-7}$

$\rho = 2 \text{ g cm}^{-3}$  for the MBA average density,  $r_1 = 4.565 \times 10^7 \text{ cm}$  for the radius of Ceres, and  $r_0 = 100 \text{ cm}$  for the smallest radius of an asteroid that is still an opaque target for incident CR particles. The central grammage in this case ( $r_0 = 100 \text{ cm}$ ) is  $\sim 400 \text{ g cm}^{-2}$ . Since the composition of the MBAs (and other SSSB populations) is mainly oxygen, this corresponds to  $\sim 5$  interaction lengths, which is sufficient for the hadronic cascade to fully develop at the CR energies we consider. With these parameters, the total MBA albedo flux is  $X = F_{\text{tot}}/F_{\text{Moon}} = 0.05, 0.67,$  and  $12$  for extrapolation to small sizes with indices  $n = 2.5, 3.0,$  and  $3.5,$  respectively (see Fig. 1).

Similarly, for the Jovian Trojan asteroids we can estimate the  $\gamma$ -ray flux assuming the same size distribution as for MBAs, but with  $l \sim 5.2 \text{ AU}$  and  $r_0 = 200 \text{ cm}$  (which gives the same central grammage for  $\rho = 1 \text{ g cm}^{-3}$ ). We obtain  $X = F_{\text{tot}}/F_{\text{Moon}} = 0.01, 0.07,$  and  $0.8$  (averaged over their orbit) for a similar extrapolation to small sizes with indices  $n = 2.5, 3.0,$  and  $3.5,$  respectively. For the closest ( $4.2 \text{ AU}$ ) and the farthest ( $6.2 \text{ AU}$ ) distances to Earth, the fluxes will be  $0.01, 0.1,$  and  $1.2,$  and  $0.006, 0.05,$  and  $0.5,$  respectively.

The KBO size distribution is known very approximately. The second largest object of the Kuiper Belt, after 136199 Eris, is Pluto,  $r_1 = 1.195 \times 10^8 \text{ cm}$ , while the majority of the KBOs are icy rocks and comets with  $\rho = 0.5 \text{ g cm}^{-3}$ . To keep the same central grammage of the smallest body,  $\sim 400 \text{ g cm}^{-2}$ , we have to use a larger minimum radius,  $r_0 = 400 \text{ cm}$ , than for the MBAs. The incident spectrum of CR particles at  $>30 \text{ AU}$  approaches the LIS spectrum, which results in a factor of  $\sim 2$  increase below  $\sim 1 \text{ GeV}$  of the albedo flux compared to the same body at  $1 \text{ AU}$  (Fig. 2). For these parameters, the total Kuiper Belt albedo flux is  $X^{\text{KBO}} = F_{\text{tot}}^{\text{KBO}}/F_{\text{Moon}} = 0.2, 34,$  and  $1168$  for  $n = 3.0, 3.5,$  and  $3.9,$  respectively. Removing Eris and Pluto ( $\sim 0.005 M_{\oplus}$  combined) from the Kuiper Belt and using Charon instead,  $r_1 = 6 \times 10^7 \text{ cm}$ , results in the flux increase:  $X^{\text{KBO}} = F_{\text{tot}}^{\text{KBO}}/F_{\text{Moon}} = 0.35, 46,$  and  $1222$  for the same values of  $n$ . However, this change is simply the result of anchoring the power-law size distribution to a large body.

Our estimates show that the albedo of MBAs and KBOs could account for the EGRET upper limit of the flux from the ecliptic. For the adopted size distributions of SSSBs ( $n = 3.0$  for MBAs and  $n = 3.5$  for KBOs), the KBO albedo is essentially brighter. However, if the MBA size distribution is somewhat steeper than our adopted index of  $n = 3.0$  (e.g., as for the distribution proposed by Cheng 2004), it can account for the total albedo flux from the ecliptic. The SSSB  $\gamma$ -ray albedo, especially of the collectively moving Trojan groups, might be responsible for some fraction of the EGRET unidentified point sources at low ecliptic latitudes.

A possible way to distinguish the albedo emission of MBAs and KBOs is to study the emission as a function of solar elongation angle. In the antisolar direction,  $\theta \approx 180^\circ$ , the direction in which the Main Belt is closest to the Earth ( $\sim 1.7 \text{ AU}$ ), the flux is predicted to be as much as  $\sim 5$  times that in the solar direction,

$\theta \approx 0^\circ$ . On the other hand, the brightness of the Kuiper Belt is only weakly dependent on the elongation angle because it is much farther away. The positions of the Trojans on the sky are known, being determined relative to their respective planet (Jupiter or Neptune), making them easier to detect.

The detection of the CR-induced  $\gamma$ -ray albedo of MBAs, Trojans, and the KBOs by  $\gamma$ -ray instruments is possible. At higher energies,  $\gtrsim 1 \text{ GeV}$ , where the  $\gamma$ -ray albedo flux is steady and does not depend on the solar modulation, it can serve as a normalization point to the cumulative brightness of all MBAs plus KBOs. At lower energies,  $\lesssim 1 \text{ GeV}$ , the component of the albedo, which is independent of elongation, the KBO albedo, will tell us directly about the LIS spectrum of CRs. Therefore, the observations of the albedo flux can provide us with valuable information about the size distributions of SSSBs in both regions, while the shape of the albedo spectrum can tell us about the LIS spectra of CR protons and helium at high energies. In turn, a detection of the MBA and KBO albedo at MeV–GeV energies will enable us to normalize properly the cumulative albedo spectrum and make a prediction for the intensity of the 511 keV line.

A conservative estimate of the 511 keV line flux from SSSBs can be made using the upper limit derived in § 4. The total flux of 511 keV photons from the Moon is  $F_{\text{Moon}}^{511} \approx 10^{-3} \Delta E \approx 2.4 \times 10^{-5} \text{ photons cm}^{-2} \text{ s}^{-1}$  (Fig. 2,  $\Phi = 0 \text{ MV}$ ), where  $\Delta E = 0.024 \text{ MeV}$  is the size of the bin containing  $E = 0.511 \text{ MeV}$ . The total flux from the SSSBs,  $X^{511} = F_{\text{tot}}^{511}/F_{\text{Moon}}^{511}$ , can be calculated from equations (7)–(11). The SSSB albedo contribution to the 511 keV line flux within the Galactic bulge is  $\sim 0.72 F_{\text{Moon}}^{511}$ , where we assumed that the FWHM of the bulge is  $\sim 10^\circ$  (Knödlseeder et al. 2005), where  $20^\circ/360^\circ \approx 0.06$ , and where we used the upper limit derived in § 4. It gives  $\sim 2 \times 10^{-5} \text{ photons cm}^{-2} \text{ s}^{-1}$ , which is about 2% of the total bulge emission as observed by *INTEGRAL*,  $(1.05 \pm 0.06) \times 10^{-3} \text{ photons cm}^{-2} \text{ s}^{-1}$  (Knödlseeder et al. 2005). Since most of the *INTEGRAL* observing time was spent on observations of the Galactic bulge and a comparatively small fraction went into observing regions above and below the Galactic plane, it is not surprising that a diffuse band near the ecliptic (the SSSB albedo) has not been found so far. It is interesting that the OSSE map of the 511 keV line has a controversial feature, the so-called annihilation fountain, above the Galactic bulge (Purcell et al. 1997), which, in fact, may be the asteroid albedo foreground instead. Note that the  $\gamma$ -ray spectrometer on the *NEAR-Shoemaker* spacecraft made observations of the 511 keV line from 433 Eros (Evans et al. 2001) on the surface of Eros itself; however, it is hard to judge the absolute intensity of the line from the published data.

Our estimates of the fluxes assume that the mass and radius distributions are valid for the whole range of masses, which is not necessarily true. The number of small bodies may be larger or smaller than the extrapolation from the distribution of more massive bodies. We have also assumed spherical bodies. However, the smallest bodies are distinctly nonspherical, which would

make them somewhat brighter than we have estimated. Thus, our calculations underestimate the SSSB albedo emission.

The bodies that are smaller than the cutoff radius ( $r_0 = 100$  cm for MBAs, 200 cm for Trojans, and 400 cm for KBOs) will also contribute to the albedo flux. Because of their smaller size, only the initial stage of the CR cascade will develop, producing a harder albedo spectrum, while its intensity will be reduced due to the partial conversion of energy of the primary CR particles into albedo  $\gamma$ -rays.

We emphasize that the detection of the  $\gamma$ -ray albedo from MBAs, KBOs, and other SSSB families directly probes the size distribution of these bodies below the detection limit of other methods, over considerably larger regions of the sky. The detectability of the  $\gamma$ -ray emission by these objects has implications for studies of the evolution of the solar and exosolar planetary systems (Brown 2004), of CRs, and of diffuse  $\gamma$ -rays. The *GLAST* Large Area Telescope (LAT),<sup>6</sup> to be launched by NASA in 2008 June, will in just one year have an essentially uniform exposure over the entire sky a factor of 40 or more deeper than EGRET and will be free from

<sup>6</sup> See the *GLAST* LAT performance Web page at <http://www-glast.slac.stanford.edu>.

sensitivity variations owing to aging of consumables. This capability will permit detection of albedo  $\gamma$ -ray fluxes for SSSBs at even the lunar flux level.

I. V. M. wishes to dedicate this paper to the memory of his mother. We thank Clark Chapman and Bill Merline for careful reading of the manuscript and insightful remarks, and Joe Burns, Alan Harris, and Ed Tedesco for sharing their thoughts. This investigation was inspired by a question from NASA Associate Administrator for the Science Mission Directorate, S. Alan Stern. I. V. M. and J. F. O. acknowledge support from a NASA Astronomy and Physics Research and Analysis Program (APRA) grant. T. A. P. acknowledges partial support from the US Department of Energy. P. F. M. acknowledges support from NASA contract NAS5-00147 for *GLAST*. This work was carried out while J. F. O. was a visiting scientist at Stanford University; he wishes to acknowledge the kind hospitality. This research has made use of data obtained through the High Energy Astrophysics Science Archive Research Center, provided by the NASA/Goddard Space Flight Center.

#### REFERENCES

- Asphaug, E., & Benz, W. 1994, *Nature*, 370, 120  
 Babich, D., Blake, C. H., & Steinhardt, C. L. 2007, *ApJ*, 669, 1406  
 Backman, D. E., Dasgupta, A., & Stencel, R. E. 1995, *ApJ*, 450, L35  
 Baltz, E. A., et al. 2008, *J. Cosmol. Astropart. Phys.*, submitted  
 Bergström, L., Ullio, P., & Buckley, J. H. 1998, *Astropart. Phys.*, 9, 137  
 Bernstein, G. M., et al. 2004, *AJ*, 128, 1364  
 Binzel, R. P., Hanner, M. S., & Steel, D. I. 1999, in *Allen's Astrophysical Quantities*, ed. A. N. Cox (New York: AIP), 315  
 Brown, M. E. 2001, *AJ*, 121, 2804  
 ———. 2004, *Phys. Today*, 57, 49  
 Cheng, A. F. 2004, *Icarus*, 169, 357  
 Dohnanyi, J. S. 1969, *J. Geophys. Res.*, 74, 2531  
 Evans, L. G., et al. 2001, *Meteoritics Planet. Sci.*, 36, 1639  
 Finkbeiner, D. P., & Weiner, N. 2007, *Phys. Rev. D*, 76, 083519  
 Gleeson, L. J., & Axford, W. I. 1968, *ApJ*, 154, 1011  
 Guessoum, N., Jean, P., & Gillard, W. 2005, *A&A*, 436, 171  
 Hartman, R. C., et al. 1999, *ApJS*, 123, 79  
 Hooper, D., Zaharijas, G., Finkbeiner, D. P., & Dobler, G. 2008, *Phys. Rev. D*, 77, 043511  
 Hunter, S. D., et al. 1997, *ApJ*, 481, 205  
 Ivezić, Ž., et al. 2001, *AJ*, 122, 2749  
 Jean, P., et al. 2006, *A&A*, 445, 579  
 Jedicke, R., & Metcalfe, T. S. 1998, *Icarus*, 131, 245  
 Jewitt, D. C., & Luu, J.-X. 1995, *AJ*, 109, 1867  
 Jewitt, D. C., et al. 2000, *AJ*, 120, 1140  
 Kenyon, S. J., & Bromley, B. C. 2004, *AJ*, 128, 1916  
 Knödseder, J., et al. 2005, *A&A*, 441, 513  
 Krasinsky, G. A., Pitjeva, E. V., Vasilyev, M. V., & Yagudina, E. I. 2002, *Icarus*, 158, 98  
 Lacerda, P., & Jewitt, D. C. 2007, *AJ*, 133, 1393  
 Langner, U. W., Potgieter, M. S., Fichtner, H., & Borrmann, T. 2006, *ApJ*, 640, 1119  
 Luu, J.-X., & Jewitt, D. C. 2002, *ARA&A*, 40, 63  
 Mann, R. K., et al. 2007, *AJ*, 134, 1133  
 Marchis, F., et al. 2006, *Nature*, 439, 565  
 Moskalenko, I. V., & Porter, T. A. 2007, *ApJ*, 670, 1467  
 ———. 2008, in *Proc. 30th Int. Cosmic Ray Conf. (Merida)*, in press  
 Moskalenko, I. V., Porter, T. A., & Digel, S. W. 2006, *ApJ*, 652, L65  
 Moskalenko, I. V., Porter, T. A., Digel, S. W., Michelson, P. F., & Ormes, J. F. 2008, in *Proc. 39th Lunar and Planetary Science Conf. (Houston: Lunar and Planetary Inst.)*, 2280  
 Orlando, E., Dirk, P., & Strong, A. W., 2007, in *AIP Conf. Proc. 921, The First GLAST Symposium*, ed. S. Ritz, P. Michelson, & C. Meegan (Melville: AIP), 502  
 Orlando, E., & Strong, A. W. 2007, *Ap&SS*, 309, 359  
 Prantzos, N. 2006, *A&A*, 449, 869  
 Ptuskin, V. S., Moskalenko, I. V., Jones, F. C., Strong, A. W., & Zirakashvili, V. N. 2006, *ApJ*, 642, 902  
 Purcell, W. R., et al. 1997, *ApJ*, 491, 725  
 Sheppard, S. S. 2005, Ph.D. thesis, Univ. of Hawaii  
 Sheppard, S. S., & Trujillo, C. A. 2006, *Science*, 313, 511  
 Solem, J. C. 1994, *Nature*, 370, 349  
 Sowards-Emmerd, D., Romani, R. W., & Michelson, P. F. 2003, *ApJ*, 590, 109  
 Sowards-Emmerd, D., Romani, R. W., Michelson, P. F., & Ulvestad, J. S. 2004, *ApJ*, 609, 564  
 Sreekumar, P., et al. 1998, *ApJ*, 494, 523  
 Stern, S. A. 2003, *Nature*, 424, 639  
 Stone, E. C., et al. 2005, *Science*, 309, 2017  
 Strong, A. W., Moskalenko, I. V., & Reimer, O. 2004, *ApJ*, 613, 956  
 Takahashi, T., Mitsuda, K., & Kunieda, H. 2006, *Proc. SPIE*, 6266, 62660D  
 Tancredi, G., Fernández, J. A., Rickman, H., & Licandro, J. 2006, *Icarus*, 182, 527  
 Tedesco, E. F., Cellino, A., & Zappalà, V. 2005, *AJ*, 129, 2869  
 Tedesco, E. F., & Desert, F.-X. 2002, *AJ*, 123, 2070  
 Thompson, D. J., Bertsch, D. L., Morris, D. J., & Mukherjee, R. 1997, *J. Geophys. Res. A*, 102, 14735  
 Toth, I. 2006, in *IAU Symp. 229, Asteroids, Comets, Meteors*, ed. D. Lazzaro, S. Ferraz-Mello, & J. Fernandez (Cambridge: Cambridge Univ. Press), 67  
 Weidenspointner, G., et al. 2006, *A&A*, 450, 1013  
 Wiegert, P., et al. 2007, *AJ*, 133, 1609  
 Yoshida, F., & Nakamura, T. 2005, *AJ*, 130, 2900  
 Yoshida, F., et al. 2003, *PASJ*, 55, 701  
 Zaharijas, G., & Hooper, D. 2006, *Phys. Rev. D*, 73, 103501





